

Mesoporous Silica Nanoparticle-Based Double Drug Delivery System for Glucose-Responsive Controlled Release of Insulin and Cyclic AMP

Yannan Zhao, Brian G. Trewyn, Igor I. Slowing, and Victor S.-Y. Lin*

Department of Chemistry, U.S. Department of Energy Ames Laboratory, Iowa State University, Ames, Iowa 50011-3111

Received March 9, 2009; E-mail: vsylin@iastate.edu

Stimuli-responsive controlled-release systems have attracted much attention for their potential applications in the area of drug and gene delivery.^{1–3} In particular, surface-functionalized, end-capped mesoporous silica nanoparticle (MSN) materials have been demonstrated as efficient stimuli-responsive controlled-release systems having the advantageous “zero premature release” property. The biocompatibility of MSN both *in vitro* and *in vivo* has been demonstrated by several recent studies.^{4–7} Furthermore, literature reports on the biodistribution and circulation properties of MSN administered in animals by intravenous injection have highlighted the promising potential of these multifunctional nanoparticles for *in vivo* biomedical applications and organ-specific delivery of therapeutics.

In contrast to nonporous nanoparticles, MSN offers both interior pore and exterior particle surfaces for loading different guest molecules. This is particularly useful for controlling the sequence of release for different cargos, which is crucial for the efficacy of many codelivery applications. These codelivery systems with control over the sequence of release could play a key role in overcoming several current challenges in therapy. For example, conventional glucose-responsive insulin delivery systems suffer from the decrease of insulin release with repeated cycles.^{8,9} This problem could be overcome if the secretion of insulin from live cells could also be induced by sequential delivery of cyclic adenosine monophosphate (cAMP), which activates Ca²⁺ channels of pancreas beta cells and hence stimulates insulin secretion.^{10,11} However, because of the poor membrane permeability of cAMP, many attempts have been made to develop cAMP analogues¹² with good membrane permeability to study the insulin secretion mechanism. Unfortunately, to the best of our knowledge, no report of intracellular cAMP delivery by any drug carriers to control insulin production has appeared in the literature.

Herein, we report on the synthesis of a glucose-responsive MSN-based double delivery system for both insulin and cAMP with precise control over the sequence of release. As depicted in Figure 1a, gluconic acid-modified insulin (G-Ins)⁸ proteins are immobilized on the exterior surface of MSN and also serve as caps to encapsulate cAMP molecules inside the mesopores of MSN. The release of both G-Ins and cAMP from MSN can be triggered by the introduction of saccharides, such as glucose. Also, we have demonstrated that the uncapped MSN can be efficiently endocytosed by live mammalian cells, leading to effective intracellular release of the cell-membrane-impermeable cAMP.

We first synthesized an aminopropyl-functionalized (1.6 mmol g⁻¹) mesoporous silica nanosphere material (AP-MSN) with an average particle diameter of 120 nm and an MCM-41-type channel-like mesoporous structure (BJH pore diameter = 2.3 nm) via a method that we previously reported.¹³ The particle size is small enough (≤200 nm) to evade rapid sequestration by phagocytotic cells of the spleen and to allow long blood circulation.¹⁴ As

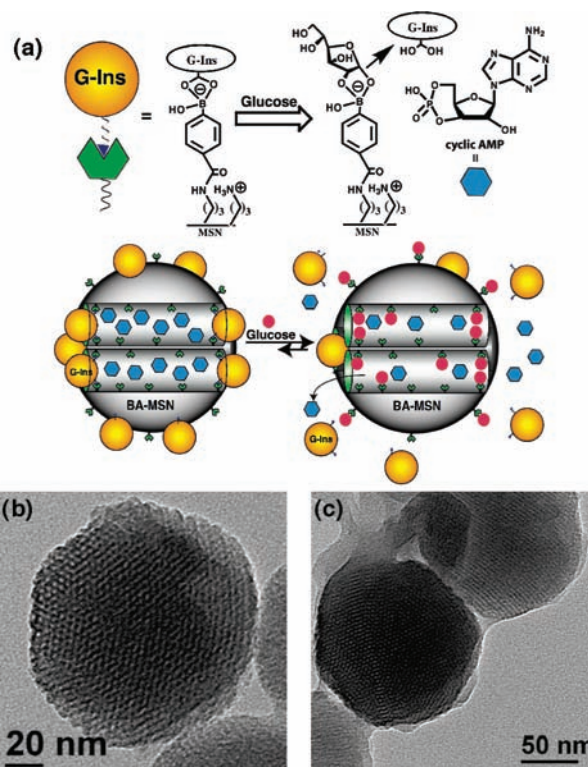


Figure 1. (a) Schematic representation of the glucose-responsive MSN-based delivery system for controlled release of bioactive G-Ins and cAMP. Transmission electron micrographs of (b) boronic acid-functionalized MSN and (c) FITC-G-Ins-capped MSN.

described in the Supporting Information (SI), 4-carboxyphenylboronic acid (0.15 g), *N*-hydroxysuccinimide (0.10 g), and 1-ethyl-3-(3-dimethylaminopropyl)carbodiimide hydrochloride (0.2 g) were introduced to AP-MSN (400 mg) in DMSO (20 mL) to yield the boronic acid-functionalized (0.5 mmol g⁻¹) MSN material (BA-MSN) (Figure 1b). The presence of both aminopropyl and phenylboronic acid groups stabilizes the formation of borates with 1,2- or 1,3-diols (Figure 1a). A fluorescein isothiocyanate (FITC)-labeled G-Ins (FITC-G-Ins) was prepared according to a literature procedure.⁸ The bioactivity of G-Ins was demonstrated to be similar to that of unmodified insulin.⁸ The mesopores of BA-MSN (100 mg) were loaded with cAMP (1 mM) in PBS buffer (10 mL, pH 7.4) and then capped with FITC-G-Ins (200 mg) through reversible covalent bonding between phenylboronic acid and the vicinal diols of FITC-G-Ins, giving rise to the desired FITC-G-Ins-MSN material (Figure 1c). The loadings of cAMP and FITC-G-Ins were determined to be 27 and 64 μmol/g by HPLC¹⁵ and fluorescence emission spectroscopy, respectively. As detailed in the SI, the structures and surface properties of BA-MSN and FITC-G-Ins-MSN

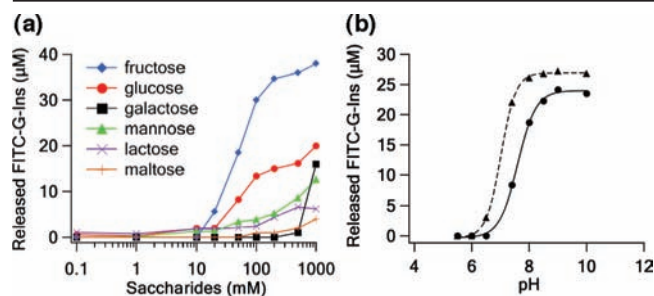


Figure 2. (a) Dependence of FITC-G-Ins release from FITC-G-Ins-MSN (2 mg mL^{-1} in PBS, pH 7.4) on the concentration of saccharide triggers. (b) pH titration of insulin release from FITC-G-Ins-MSN (2 mg mL^{-1} in PBS) triggered by 50 mM glucose (solid line) and 50 mM fructose (dashed line).

were characterized by powder X-ray diffraction (XRD), N_2 surface analysis, ζ potential measurements, and transmission electron microscopy.

As demonstrated in the literature,¹⁶ phenylboronic acid forms much more stable cyclic esters with the adjacent diols of saccharides than with acyclic diols. This means that the linkage between FITC-G-Ins and BA-MSN could be cleaved by introducing various saccharides. Therefore, it was expected that the release of FITC-G-Ins would be sensitive to the chemical structures and concentrations of different carbohydrate triggers in forming stable cyclic boronic esters with BA-MSN. Among different saccharide triggers, the release of FITC-G-Ins indeed showed a strong preference for fructose, followed by glucose, as shown in Figure 2a. The observed high selectivity for fructose is consistent with other reported monoboronic acid-based sensors for saccharide recognition.¹⁷ It is known that saccharides can interconvert between their pyranose and furanose isomeric forms, and phenylboronic acid has a strong preference for binding with the hydroxyls of saccharides in their furanose forms. The high selectivity toward fructose could be explained by its high percentage of furanose form in water (25% for fructose vs 0.14% for glucose).¹⁸

For monoboronic acids in water with 1:1 saccharide/boronic acid complexation, high selectivity for fructose and low selectivity for glucose were observed, and the difference was attributed to the relative percentage of the furanose forms of these carbohydrates.¹⁸ Interestingly, our system was highly responsive toward fructose and glucose in comparison with other saccharides (Figure 2a). This could be attributed to the heterogeneous spacing of boronic acid groups, which leads to the coexistence of 1:1 and 1:2 complexation, where the 1:2 complexation is widely used in the design of diboronic acid systems for selective glucose sensing.¹⁹ In contrast, disaccharides (lactose and maltose) were not able to adopt a furanose form and hence could not serve as effective triggers for pore uncapping. While a stronger preference for fructose than for glucose was observed, the FITC-G-Ins-MSN system is still suitable for glucose-responsive insulin release because of the much lower level of blood fructose ($\leq 0.1 \text{ mM}$) than of glucose ($\geq 10 \text{ mM}$) in diabetic patients.

The release of FITC-G-Ins triggered by any of the saccharides was found to be complete within 30 min, which is within the time frame of normal insulin secretion. The complexation of fructose and glucose with phenylboronic acid and the corresponding release of FITC-G-Ins exhibited a strong pH dependence. As shown in Figure 2b, the release of FITC-G-Ins triggered by 50 mM fructose reached 85% of maximum release at pH 7.4. In contrast, significant release of FITC-G-Ins was observed only at pH values above 8 in the case of glucose. This is likely due to the fact that the formation of tetrahedral borate intermediate requires a pH higher than the

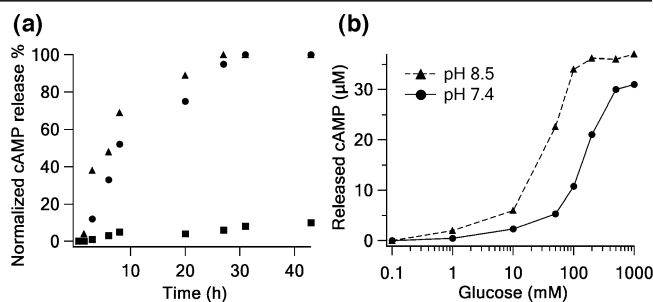


Figure 3. Controlled release of cAMP from FITC-G-Ins-MSN (2 mg mL^{-1} in PBS) (a) triggered by 50 mM glucose at pH 7.4 (●) and 8.5 (▲), with control data at pH 7.4 in the absence of glucose (■), and (b) triggered by different concentrations of glucose at pH 7.4 (solid line) and 8.5 (dashed line) measured 48 h after glucose treatment.

pK_a of boronic acid. The observed pH dependence in our material, which is indicative of the controlled release mechanism, is consistent with those of other literature-reported insulin delivery systems.²⁰

To further examine the applicability of this system, FITC-G-Ins released by a stepwise treatment of glucose at two diabetic levels (50 and 100 mM) was monitored (Figure S6 in the SI). A typical decrease in insulin release after the second cycle was observed. However, this problem of decreasing insulin level could be overcome by delivering the cell-membrane-impermeable cAMP into the cytosol to stimulate insulin secretion from pancreas beta cells. This double-release system sets up a new model for self-regulated insulin-releasing devices.

The glucose-triggered release of cAMP by FITC-G-Ins uncapping was determined by HPLC¹⁵ at pH 7.4 and 8.5, as shown in Figure 3. In PBS (pH 7.4), the cAMP-loaded FITC-G-Ins-MSN exhibited less than 10% leaching in the absence of glucose trigger, suggesting a good capping efficiency of FITC-G-Ins. The rate of cAMP release triggered by 50 mM glucose at pH 7.4 and 8.5 showed similar diffusion-controlled kinetic profiles. Specifically, ~80% of total release was obtained within 20 h. Furthermore, 55 and 67% of the total loaded cAMP ($27 \mu\text{mol g}^{-1}$) were released after 30 h at pH 7.4 and 8.5, respectively (Figure 3a). As shown in Figure 3b, the release of cAMP strongly depends on the concentration of glucose. A significant cAMP release at pH 7.4 was observed when the concentration of glucose trigger was above 100 mM, whereas 50 mM glucose triggered almost 60% of maximum release at pH 8.5. This pH dependence of cAMP release is consistent with that of FITC-G-Ins release from MSN.

To correlate these *in vitro* results with the physiological concentrations for potential *in vivo* applications, the therapeutic dosage of this material was estimated. Between meals, the insulin level typically rises from a fasting level of 20–30 pM to a 30 min maximum of 250–300 pM, depending upon the amount and quality of carbohydrates consumed, while the diabetic insulin level remains at 20–30 pM or below. It has been reported in the literature that at least 250–300 pM of insulin is needed to decrease the diabetic blood glucose concentration to the normal level.²¹ Our results indicate that 20 mM glucose indeed induced the release of $2 \mu\text{M}$ G-Ins from our material at a concentration of 2 mg mL^{-1} (Figure 2a). Delivery of 250–300 pM of G-Ins would require only $0.25\text{--}0.3 \mu\text{g mL}^{-1}$ MSN material, which is 4 orders of magnitude lower in concentration than what we have demonstrated above. As reported previously, the MSN dosage has a minimal effect on viability and proliferation of mammalian cells at concentrations below $100 \mu\text{g mL}^{-1}$ after 6 days.²² Also, the maximum concentration of cAMP released from 2 mg mL^{-1} G-Ins-MSN was $30 \mu\text{g mL}^{-1}$ (Figure 3b). On the basis of these results, we envision that the application of $0.25\text{--}0.30 \mu\text{g mL}^{-1}$ G-Ins-MSN *in vivo* could sufficiently deliver

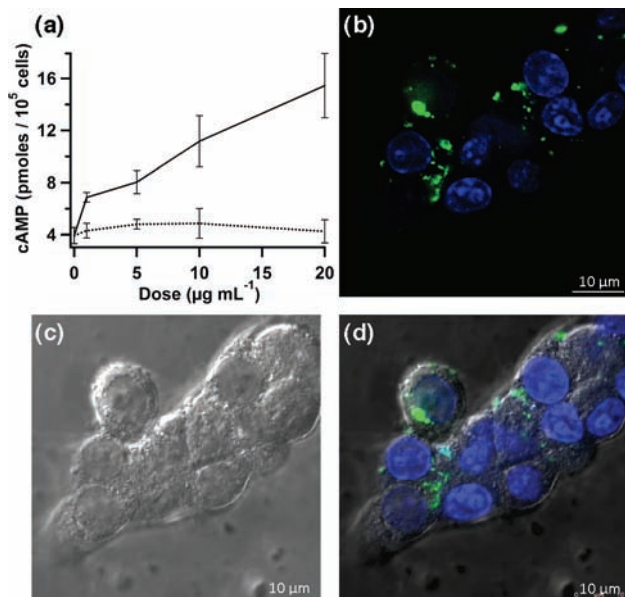


Figure 4. (a) Intracellular cAMP concentration of rat pancreatic RIN-5F cells treated with the cAMP-loaded BA-MSN (solid line) and free-solution cAMP (dashed line), measured after 6 h of introduction. (b) Fluorescence confocal micrograph of RIN-5F cells incubated with $20 \mu\text{g mL}^{-1}$ Fluo-cAMP-loaded BA-MSN (green) for 6 h. Cell nuclei were stained with DAPI (blue). (c) Corresponding differential interference contrast (DIC) micrographs. (d) Fluorescence confocal and DIC merged image. Enlarged individual and merged images are shown in Figure S9 in the SI.

both G-Ins and cAMP for blood glucose regulation and insulin secretion, respectively, and would not produce any acute toxic effects.

To examine the cytotoxicity of the cAMP-loaded G-Ins-MSN material, cell viability and proliferation profiles of four different cell lines [rat pancreatic islet tumor (RIN-5F), mouse liver, skin fibroblast, and human cervical cancer (HeLa) cells] were evaluated by Guava ViaCount cytometry assay after 24 h inoculation with the material. Good cell viability (>90%) and proliferation (>80%) were observed for all cell lines containing 5 or $20 \mu\text{g mL}^{-1}$ G-Ins-MSN. These results further indicate that this MSN-based double delivery system is biocompatible.

The cellular uptake properties of the cAMP-loaded BA-MSN with and without G-Ins capping were investigated with RIN-5F cells. As detailed in the SI, BA-MSN labeled with FITC (FITC-BA-MSN) for this study was prepared prior to cAMP loading and G-Ins capping. The endocytosis efficiency was quantified by flow cytometry after 1 h of incubation with each material at $10 \mu\text{g mL}^{-1}$ (Figure S8). Interestingly, the cAMP-loaded FITC-BA-MSN without G-Ins capping showed a 2-fold higher endocytosis efficiency than that of the G-Ins-capped material. The result could be attributed to the difference in their surface charge properties: the ζ potentials were -28.3 mV for the uncapped material and -44.5 mV for the G-Ins-capped version.¹³ This difference between the endocytosis efficiencies of the capped and uncapped materials implies that G-Ins-MSN could circulate in the regulatory system before the glucose-induced G-Ins release, and the enhanced cellular uptake of cAMP-loaded BA-MSN after the pore uncapping would allow efficient intracellular cAMP delivery.

To quantify the degree of intracellular release of cAMP from our system, the cAMP-loaded BA-MSN was allowed to be internalized by RIN-5F cells. After 6 h of incubation, the total cellular concentration of cAMP was measured using a Millipore cAMP HTS immunoassay (see the SI). The result was compared

with that of RIN-5F cells introduced to free-solution cAMP. As shown in Figure 4a, the total cellular concentration of cAMP indeed increased proportional to the dosage of cAMP-loaded BA-MSN. In contrast, no significant elevation of the cellular concentration of cAMP was observed in the case of free-solution cAMP, even at the high dosage of $20 \mu\text{g mL}^{-1}$, which is consistent with the poor cell-membrane permeability of free-solution cAMP.

To visualize intracellular delivery of cAMP, a membrane impermeable, fluorescence-labeled cAMP (8-Fluo-cAMP)²³ was loaded into the BA-MSN. Fluo-cAMP-loaded BA-MSN ($20 \mu\text{g mL}^{-1}$) was incubated with RIN-5F cells for 6 h. The fluorescence confocal micrographs (Figure 4b–d) clearly showed that Fluo-cAMP-loaded BA-MSN was indeed internalized by live RIN-5F cells. Green fluorescence was observed for both Fluo-cAMP-loaded BA-MSN particles and the free Fluo-cAMP molecules released from the MSN intracellularly.

In conclusion, we have successfully demonstrated that phenylboronic acid-functionalized MSN can serve as an efficient code-delivery system for saccharide-responsive controlled release of insulin and cAMP. The good biocompatibility, cellular uptake properties, and efficient intracellular release of cAMP set up the basis for future in vivo controlled-release biomedical applications.

Acknowledgment. This research was supported by the U.S. National Science Foundation (CHE-0809521).

Supporting Information Available: Synthesis and characterization of AP-MSN, BA-MSN, and FITC-G-Ins-MSN; cell viability and proliferation assays; and flow cytometry, intracellular cAMP quantification, and confocal fluorescence microscopy studies. This material is available free of charge via the Internet at <http://pubs.acs.org>.

References

- (1) For a review, see: Slowing, I. I.; Vivero-Escoto, J. L.; Wu, C.-W.; Lin, V. S. Y. *Adv. Drug Delivery Rev.* **2008**, *60*, 1278.
- (2) For a review, see: Descalzo, A. B.; Martinez-Manez, R.; Sancenon, F.; Hoffmann, K.; Rurack, K. *Angew. Chem., Int. Ed.* **2006**, *45*, 5924.
- (3) For a review, see: Angelos, S.; Liang, M.; Choi, E.; Zink, J. I. *Chem. Eng. J. (Amsterdam, Neth.)* **2008**, *137*, 4.
- (4) Lee, C.-H.; Cheng, S.-H.; Wang, Y.-J.; Chen, Y.-C.; Chen, N.-T.; Souris, J.; Chen, C.-T.; Mou, C.-Y.; Yang, C.-S.; Lo, L.-W. *Adv. Funct. Mater.* **2009**, *19*, 215.
- (5) Slowing, I. I.; Wu, C.-W.; Vivero-Escoto, J. L.; Lin, V. S. Y. *Small* **2009**, *5*, 57.
- (6) Taylor, K. M. L.; Kim, J. S.; Rieter, W. J.; An, H.; Lin, W.; Lin, W. *J. Am. Chem. Soc.* **2008**, *130*, 2154.
- (7) Wu, S.-H.; Lin, Y.-S.; Hung, Y.; Chou, Y.-H.; Hsu, Y.-H.; Chang, C.; Mou, C.-Y. *ChemBioChem* **2008**, *9*, 53.
- (8) Shiino, D.; Kataoka, K.; Koyama, Y.; Yokoyama, M.; Okano, T.; Sakurai, Y. *J. Intell. Mater. Syst. Struct.* **1994**, *5*, 311.
- (9) Shiino, D.; Murata, Y.; Kubo, A.; Kim, Y. J.; Kataoka, K.; Koyama, Y.; Kikuchi, A.; Yokoyama, M.; Sakurai, Y.; Okano, T. *J. Controlled Release* **1995**, *37*, 269.
- (10) Charles, M. A.; Fanska, R.; Schmid, F. G.; Forsham, P. H.; Grodsky, G. M. *Science* **1973**, *179*, 569.
- (11) Dyachok, O.; Idevall-Hagren, O.; Saagtorp, J.; Tian, G.; Wuttke, A.; Arriemerlou, C.; Akusjaervi, G.; Gylfe, E.; Tengholm, A. *Cell Metab.* **2008**, *8*, 26.
- (12) Schultz, C.; Vajanaphanich, M.; Genieser, H.-G.; Jastorff, B.; Barrett, K. E.; Tsieng, R. Y. *Mol. Pharmacol.* **1994**, *46*, 702.
- (13) Slowing, I.; Trewyn, B. G.; Lin, V. S. Y. *J. Am. Chem. Soc.* **2006**, *128*, 14792.
- (14) Awasthi, V. D.; Garcia, D.; Goins, B. A.; Phillips, W. T. *Int. J. Pharm.* **2003**, *253*, 121.
- (15) Hoewer, H.; Zoch, E. *Fresenius' Z. Anal. Chem.* **1987**, *327*, 555.
- (16) Springsteen, G.; Wang, B. *Tetrahedron* **2002**, *58*, 5291.
- (17) Phillips, M. D.; James, T. D. *J. Fluoresc.* **2004**, *14*, 549.
- (18) Lorand, J. P.; Edwards, J. O. *J. Org. Chem.* **1959**, *24*, 769.
- (19) Fang, H.; Kaur, G.; Wang, B. *J. Fluoresc.* **2004**, *14*, 481.
- (20) Matsumoto, A.; Ikeda, S.; Harada, A.; Kataoka, K. *Biomacromolecules* **2003**, *4*, 1410.
- (21) Suckale, J.; Solimena, M. *Front. Biosci.* **2008**, *13*, 7156.
- (22) Radu, D. R.; Lai, C.-Y.; Jiftinija, K.; Rowe, E. W.; Jiftinija, S.; Lin, V. S. Y. *J. Am. Chem. Soc.* **2004**, *126*, 13216.
- (23) Moll, D.; Prinz, A.; Brendel, C. M.; Berrera, M.; Guske, K.; Zaccolo, M.; Genieser, H.-G.; Herberg, F. W. *BMC Biochem.* **2008**, *9*, 18.

JA901831U